Protein Structures

DOI: 10.1002/anie.200903771

Unfolded-State Structure and Dynamics Influence the Fibril Formation of Human Prion Protein**

*Christian Gerum, Robert Silvers, Julia Wirmer-Bartoschek, and Harald Schwalbe**

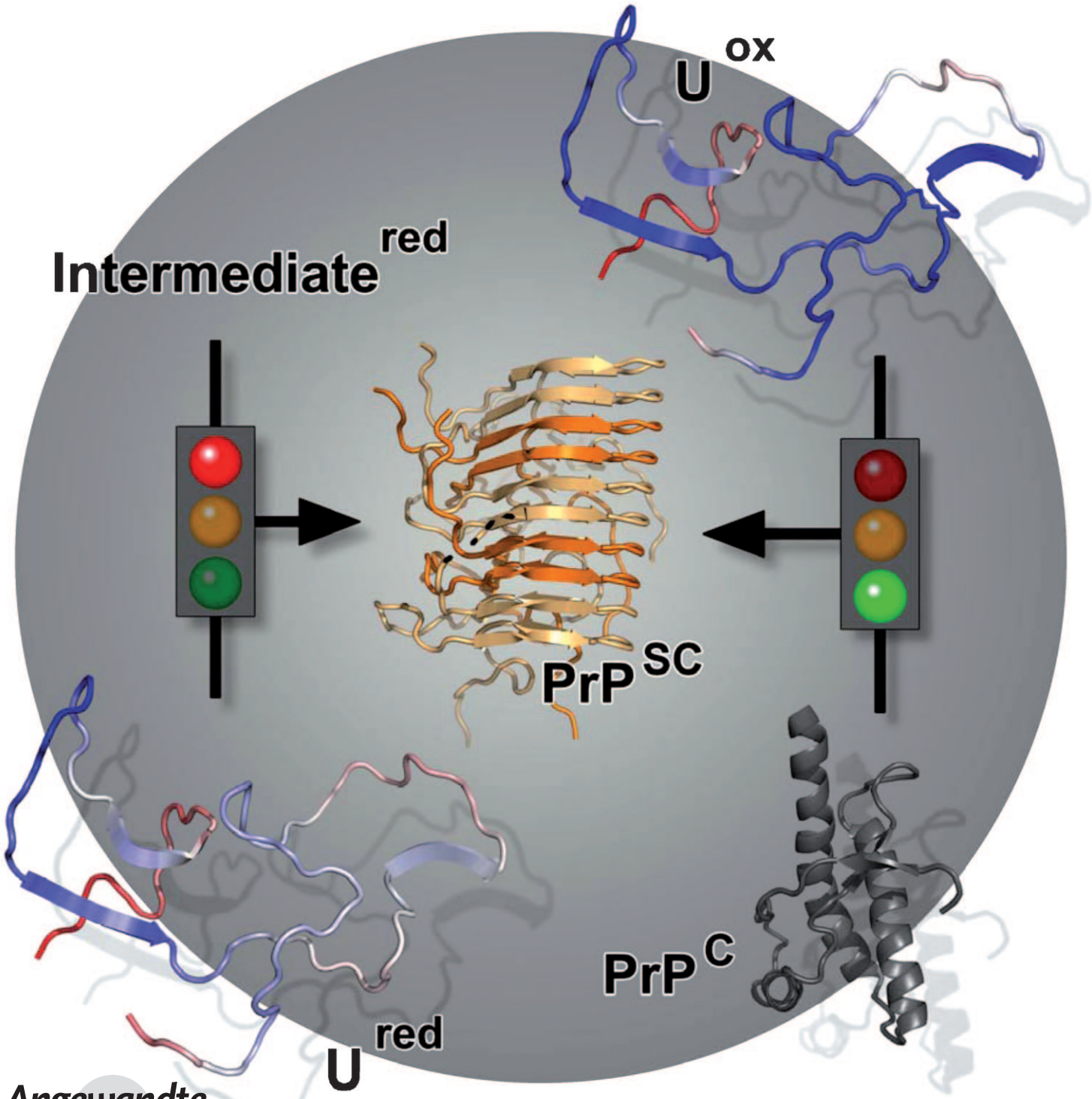

Transmissible spongiform encephalopathies are characterized by the accumulation of the abnormal "scrapie" form (PrP^{Sc}) of the endogenous cellular form (PrP^{C}) of the prion protein (PrP) in the brain. The conversion of soluble PrP^{C} into the pathogenic form involves large-scale rearrangement of the tertiary structure to convert the native benign state of the protein into a highly ordered fibril aggregate. The cellular protein PrP^{C} and the abnormal isoform of the protein PrP^{Sc} have very different three-dimensional structures. While PrP^{C} has substantial amount (40%) of α-helices,[1] models of PrP^{Sc} suggest a β-sheet superstructure in the fibrillar state.[2] PrP^{C} is a soluble monomer and sensitive to proteases, whereas PrP^{Sc} builds up insoluble oligomeric amyloid structures and is partially protease resistant.[3] The native structure of the C-terminal domain (amino acid 121 to 230) of human PrP (hPrP) contains three α-helices and a short antiparallel β-sheet.[4] The N-terminal domain (amino acid 23 to 120) is very flexible with no ordered structure.[5,6] Native structures of disease-related point mutants and of prion proteins from other species have identical overall fold with only very localized differences in the structures.[7,8] Besides the amyloid, a second oligomeric structure with significant β-sheet structure, the so called β-oligomer, can be formed at pH 3.6 in the presence of 1 M urea or GdmCl.[9]

The conversion of PrP^{C} into PrP^{Sc} occurs posttranslationally.[10] It was long speculated that the β-oligomer is an on pathway intermediate for the formation of the amyloid. However, it was shown that the β-oligomer has to disassemble completely to a monomeric species before forming an amyloid.[11] Therefore, intermediates that are at least partially unfolded are present during fibril formation, but the detailed mechanism of this conversion including the influence of disease-related mutations remains unknown.

We investigated the unfolded state of the prion protein as the third important conformational state besides the native state and the fibril aggregate. Structure and dynamics of the urea-denatured states of the C-terminal domain of the human prion protein hPrP(121–230) both in the oxidized ($hPrP^{ox}$) and in the reduced form ($hPrP^{red}$) have been investigated using NMR spectroscopy. The unfolded state is monomeric as is the unknown intermediate on the pathway to prion formation. Circular dichroism (CD) and NMR spectroscopic data reveal that urea-denatured states of $hPrP^{ox}$ and $hPrP^{red}$ (8 M urea, pH 2.0, 25 °C) are largely unstructured. We observe the typical decreased dispersion of chemical shift values and narrow line width in [^{1}H,^{15}N]-HSQC NMR spectra for unfolded proteins (see Figure S1 and S2 in the Supporting Information). Urea-induced denaturation of $hPrP^{ox}$ at pH 2.0 proceeds with a relative broad transition (Supporting Information, Figure S3). The midpoint of denaturation of $hPrP^{ox}$ is at a urea concentration of 3.3 M, denaturation is complete at 8 M urea.

Figure 1 shows chemical shift differences from random coil chemical shifts[12,13] and secondary structure propensities[14] obtained from $^{13}C_{\alpha}$ and $^{13}C_{\beta}$ chemical shifts for $hPrP^{ox}$ and $hPrP^{red}$ in 8 M urea. The analysis reveals structural preferences in the unfolded state that are different compared to the locations of secondary structure in the native state of hPrP. While the native state contains a high fraction of α-helical structure elements, the propensity for residual α-helical structure is very low in the urea denatured protein, both in the oxidized and reduced state. The region (Tyr_{157}-Pro_{165}) of the second β-strand present in native PrP^{C} (β_2: Val_{161}–Arg_{164}) reveals β-strand propensity of around 10%. In addition, the region between the amino acids comprising the β_1 region and the α_1 region of the native state (Ser_{135}–Gly_{142}) shows 10% β-structure propensity. A third area with marked chemical shift deviations from random coil values in all chemical shifts is found at the terminus of the second α-helix (Ile_{182}–Val_{189}) with propensities around 7%. The SSP-formalism also predicts β-propensity for the very C-terminus of the protein, arising from the large deviation of the last residue from random coil values. This deviation is due to the terminus of the protein, rather than to real structural preferences of the residues before the last one.

We investigated the conformational dynamics by measuring ^{15}N transverse (R_2) and rotating-frame spin-lattice ($R_{1\rho}$) relaxation rates of $hPrP^{ox}$ and $hPrP^{red}$ (Figure 2).

No differences are observed between R_2 and $R_{1\rho}$ rates revealing that μs dynamics are largely absent in the unfolded states of hPrP. Based on the differences between experimental and predicted relaxation rates, regions in the polypeptide backbone can be identified that are more rigid than expected for an ideal random polypeptide chain undergoing segmental motions.[15] In $hPrP^{ox}$, the largest deviations occur around the two cysteine residues, Cys_{179} and Cys_{214}, involved in the disulfide bridge. We conclude that the native disulfide bridge imposes motional restrictions to the regions around the cysteine residues. These deviations are larger than the decrease of flexibility expected by the formation of a covalent bond between the cysteine residues, which is depicted by the gray line in the graph (Figure 2).[16] In addition, four clusters of deviating R_2 relaxation rates are found consistently for both $hPrP^{ox}$ and $hPrP^{red}$; 1) between Gly_{127} and Gly_{131} centered around Met_{129}, 2) between Ser_{135} and Gly_{142} around isoleucine residues Ile_{138} and Ile_{139}, 3) between Ser_{143} and Arg_{156} around the two hydrophobic aromatic residues Tyr_{149} and Tyr_{150}, and 4) between Asn_{159} and Tyr_{169} around tyrosines Tyr_{162} and Tyr_{163}. The most pronounced differences in dynamics between $hPrP^{ox}$ and $hPrP^{red}$ are observed around the two cysteine residues, Cys_{179} and Cys_{214}. In the reduced form, loss of motional restrictions leads to increased dynamics around these two cysteine residues and additional hydrophobic clusters remain as indicated in Figure 2: these clusters are 5) between Asn_{178} and Thr_{193}, 6) between Phe_{198} and

[*] C. Gerum, R. Silvers, Dr. J. Wirmer-Bartoschek, Prof. Dr. H. Schwalbe
Institute of Organic Chemistry and Chemical Biology
Center for Biomolecular Magnetic Resonance
Johann Wolfgang Goethe-Universität, 60438 Frankfurt (Germany)
Fax: (+49) 69-798-29515
E-mail: schwalbe@nmr.uni-frankfurt.de

[**] The work has been supported by the EU-funded projects UPMAN and EU-NMR and by the DFG-funded Cluster of Excellence: Macromolecular Complexes. The Center for Biomolecular Magnetic Resonance is funded by the state of Hesse. The authors acknowledge valuable discussion with S. Hornemann and V. Dötsch.

Supporting information for this article is available on the WWW under http://dx.doi.org/10.1002/anie.200903771.

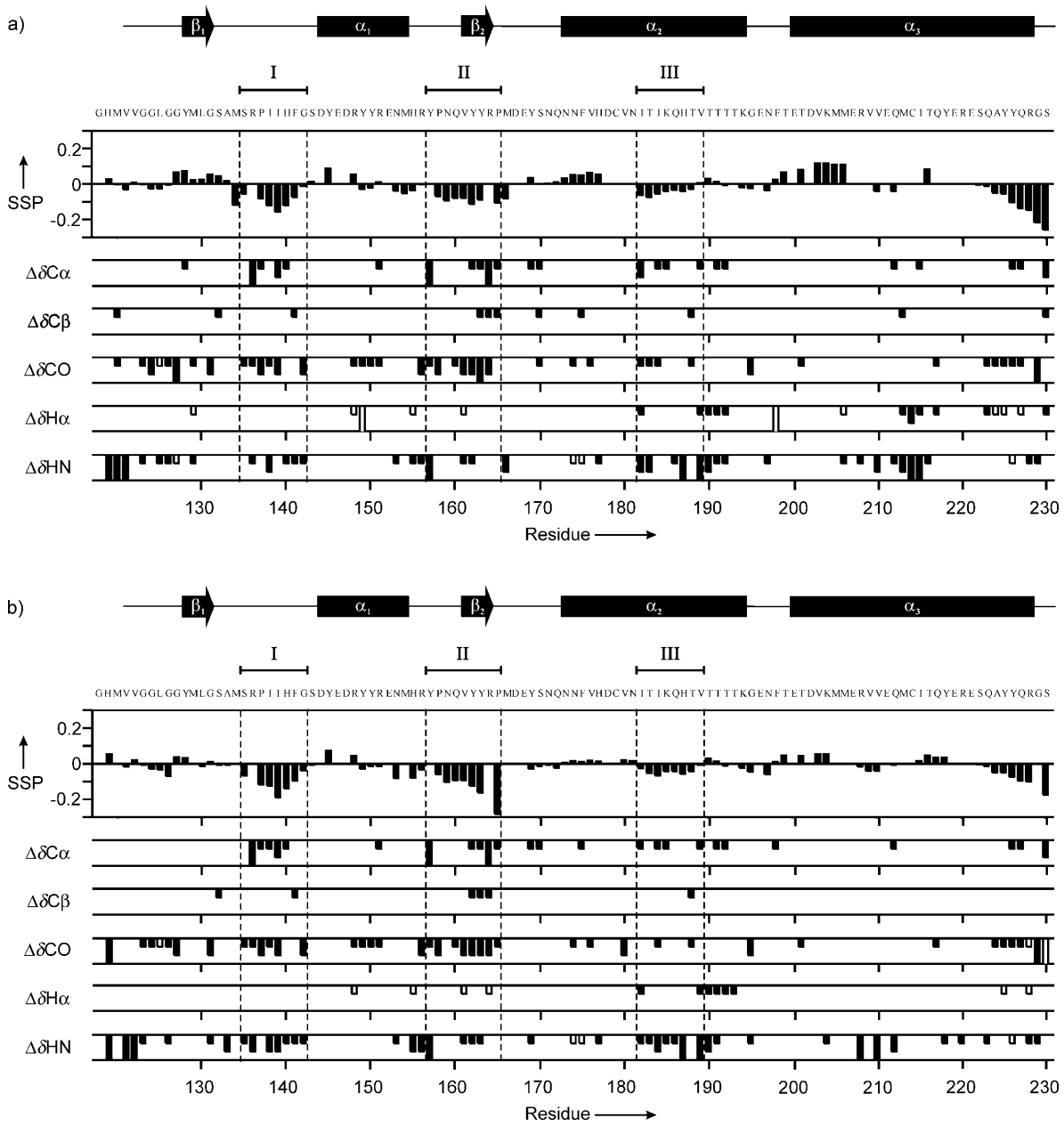

Figure 1. Secondary structure propensities (SSP)[14] and normalized secondary chemical shifts for a) $hPrP^{ox}$ and b) $hPrP^{red}$ as a function of residue number recorded in the denatured state at 8 M urea, pH 2.0, 25 °C. Deviations in chemical shifts were calculated by subtracting the measured chemical shifts from sequence corrected random coil values[12,13] for all the residues in urea-denatured $hPrP^{ox}$ and $hPrP^{red}$, respectively. Significant C_α, C_β, and CO ($|\Delta\delta| > 0.35$ ppm by 1 unit, $|\Delta\delta| > 0.7$ ppm by 2 units and $|\Delta\delta| > 1.05$ ppm by 3 units), and significant H_α and H^N ($|\Delta\delta| > 0.1$ ppm by 1 unit, $|\Delta\delta| > 0.2$ ppm by 2 units and $|\Delta\delta| > 0.3$ ppm by 3 units) secondary chemical shifts are indicated by vertical bars. Black bars indicate β-structural preferences, white bars indicate α-structure. Regions of increased β-propensities are labeled I–III, the native secondary structure elements and the sequence are indicated on top of each figure.

Met_{213}, and 7) between Ile_{215} and Gln_{227}. The locations of the clusters agree only in part with predictions made by AABUF[17] and could therefore not have been predicted from the primary sequence.

We tested whether the differences in conformational dynamics in the unfolded state of $hPrP^{ox}$ and $hPrP^{red}$ lead to differences in the fibril formation behavior monitored by thioflavin T (ThT) fluorescence (Figure 3). For the oxidized $hPrP^{ox}$, ThT fluorescence intensity increases immediately after adding the fibril-formation buffer indicating fibril formation of $hPrP^{ox}$ occurs monoexponentially.[18,19] Analysis of fluorescence kinetics at several $hPrP^{ox}$ concentrations ranging from 5 μM to 15 μM reveals second-order kinetics (see Figure S4 in the Supporting Information). By contrast, incubation of $hPrP^{red}$ does not influence the ThT fluorescence signal, no fibrils are formed. To our knowledge, this behavior has not been reported for human prion protein, but similar results were found for another amyloid forming protein, β_2-

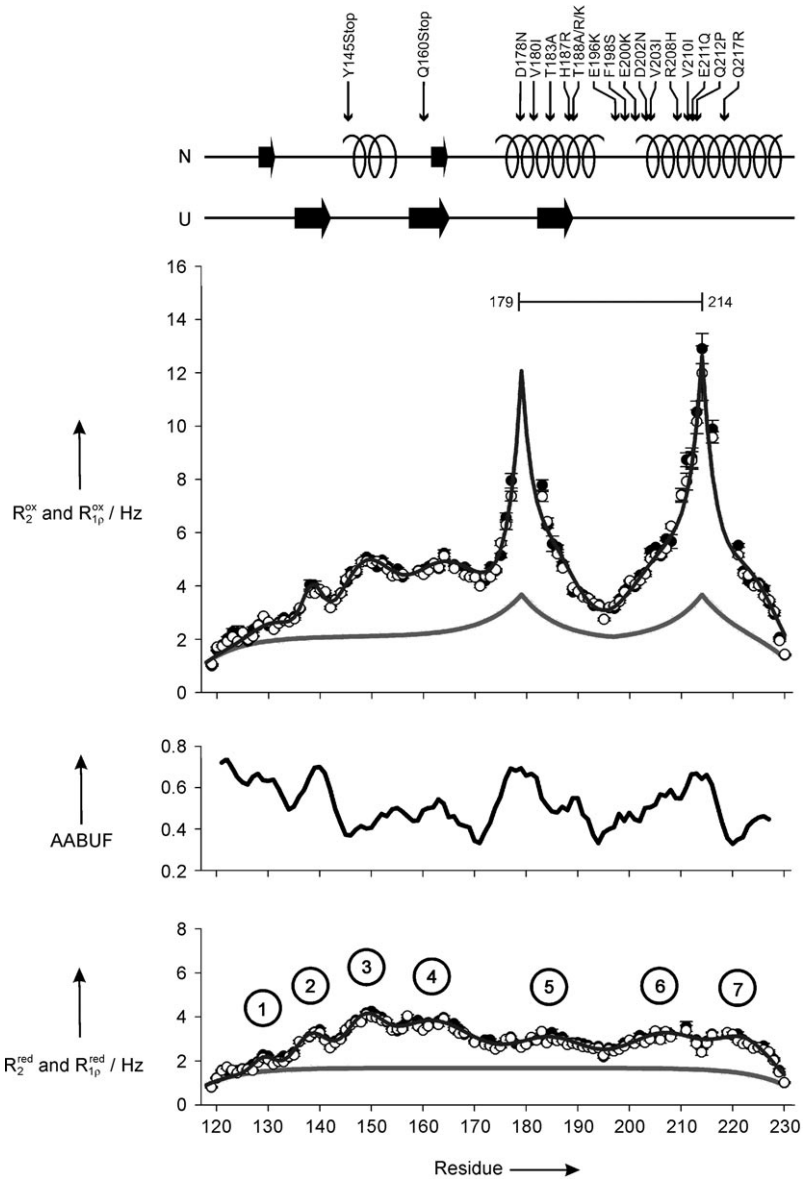

Figure 2. Dynamics of $hPrP^{ox}$ and $hPrP^{red}$. ^{15}N R_2 (black circles) and $R_{1\rho}$ relaxation rates (white circles) of $hPrP^{ox}$ (upper picture) and $hPrP^{red}$ (lower picture) in 8 M urea, pH 2.0, 25 °C are shown. Relaxation rates (R_2^{rc}) expected for a random coil ($R_{int}^{ox} = 0.17\ s^{-1}$, $\lambda_0^{ox} = 7$, $R_{int}^{red} = 0.15\ s^{-1}$ and $\lambda_0^{red} = 7$) and fitted relaxation rates are shown by a gray and black line, respectively (for detailed information, see Supporting Information). The average area buried upon folding (AABUF),[17] native secondary structure elements (N), residual structures found here (U), and point mutations associated with diseases are shown.[28,29] Additional disease-related point mutations exist in the truncated part. ①–⑦ indicate clusters or residues discussed in the main text.

microglobulin, in which the disulfide bond has been reported to be essential for amyloid fibril formation.[20] Our observations for the unfolded states of hPrP are supported by previous reports indicating that preservation of the disulfide bond is important in the conversion of PrP^C into PrP^{Sc}.[21,22]

In summary, we have investigated the urea denatured state of the cysteine oxidized and reduced state of hPrP as model of the fibril-forming intermediate of the human prion protein. Using chemical shift analysis, three areas with propensities (ca. 10%) to form β-structure (region I: Ser_{135}-Gly_{142}, region II: Tyr_{157}-Pro_{165}, region III: Ile_{182}-Val_{189}) were identified, both in the oxidized and in the reduced protein. Not revealed by analysis of chemical shifts, dramatic differences in the conformational dynamics localized around the disulfide bridge exist for the oxidized and reduced state of hPrP. These differences in conformational dynamics are linked to the observation that only $hPrP^{ox}$ forms fibrils.

The propensity to form β-strand structural elements in the unfolded state coincides with the β-multimer, in which β-sheet characteristics were found using CD spectroscopy,[9] as well with the β-sheet architecture of the human prion protein amyloid.[23,24] The NMR spectroscopy investigations presented herein allow the location of the region in the urea denatured state which has β-strand structural preferences. Interestingly, the first area with β-propensity (Ser_{135}–Gly_{142}) contains the bulky, apolar, and highly surface-exposed Ile_{138}-Ile_{139}-His_{140}-Phe_{141} sequence considered as an ideal anchor-point for initial intermolecular contacts leading to oligomerization and aggregation.[25,26] The third area with β-sheet propensity (Ile_{182}–Val_{189}) moreover is found in the recently identified core of the amyloid, comprising residues Gln_{160}–Lys_{220} made of parallel in register β-sheets.[23,24] This core agrees remarkably well with the area around the disulfide bridge, where motions are drastically restricted in the oxidized protein and large differences in the relaxation rates are observed compared to the non-amyloid-forming reduced state of the protein. We therefore propose that the unfolded state with intact

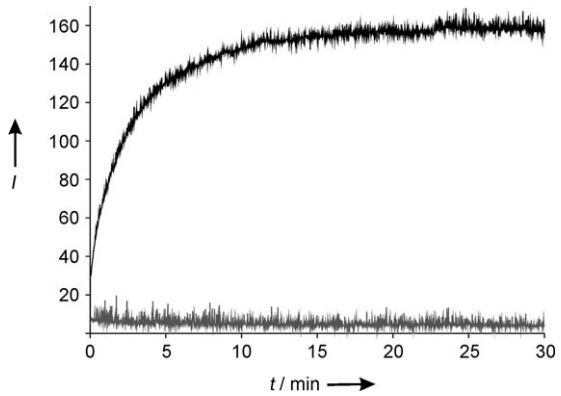

Figure 3. ThT aggregation kinetics of $hPrP^{ox}$ and $hPrP^{red}$. Experiments monitoring time-dependent fibril formation were carried out at 25 °C in a solution containing 0.5 M urea, 0.5 M GdmCl, 25 μM ThT, pH 2.0, and a final protein concentration of 15 μM. The black line indicates the aggregation behavior of $hPrP^{ox}$, the gray line of $hPrP^{red}$.

disulfide bond has features resembling the amyloid-forming intermediate, particular in the region most likely central to amyloid formation. This notion is further supported by recent ϕ-value refolding studies by Hart et al. identifying the same region as the folding nucleus in the formation of the native state of the protein, which is drastically perturbed by certain mutations leading to the formation of aberrant conformation.[27] The location of the native disulfide moreover correlates with a hotspot of inherited human prion disease-related mutations (see Figure 2):[28] 17 out of the 25 disease-related mutations are found between residue 178 and residue 217 of the protein. We propose the following hypothesis: differences in the conformational dynamics around the disulfide bridge in the unfolded state of the protein could modulate the tendency of $hPrP^{ox}$ to form fibrils, investigations to test this are ongoing.

Received: July 9, 2009
Revised: August 21, 2009
Published online: October 30, 2009

Keywords: conformational dynamics · human prion protein · NMR spectroscopy · protein structures

[1] K.-M. Pan, M. Baldwin, J. Nguyen, M. Gasset, A. Serban, D. Groth, L. Mehlhorn, Z. Huang, R. J. Fletterick, F. E. Cohen, S. B. Prusiner, *Proc. Natl. Acad. Sci. USA* **1993**, *90*, 10962.
[2] J. Safar, P. P. Roller, D. C. Gajdusek, C. J. Gibbs, *Protein Sci.* **1993**, *2*, 2206.
[3] M. P. McKinley, D. C. Bolton, S. B. Prusiner, *Cell* **1983**, *35*, 57.
[4] R. Zahn, A. Liu, T. Lührs, R. Riek, C. von Schroetter, F. L. Garcia, M. Billeter, L. Calzolai, G. Wider, K. Wüthrich, *Proc. Natl. Acad. Sci. USA* **2000**, *97*, 145.
[5] D. G. Donne, J. H. Viles, D. Groth, I. Mehlhorn, T. L. James, F. E. Cohen, S. B. Prusiner, P. E. Wright, H. J. Dyson, *Proc. Natl. Acad. Sci. USA* **1997**, *94*, 13452.
[6] R. Riek, S. Hornemann, G. Wider, M. Billeter, R. Glockshuber, K. Wüthrich, *Nature* **1996**, *382*, 180.
[7] F. Lopez Garcia, R. Zahn, R. Riek, K. Wüthrich, *Proc. Natl. Acad. Sci. USA* **2000**, *97*, 8334.
[8] D. A. Lysek, C. Schorn, L. G. Nivon, V. Esteve-Moya, B. Christen, L. Calzolai, C. von Schroetter, F. Fiorito, T. Herrmann, P. Güntert, K. Wüthrich, *Proc. Natl. Acad. Sci. USA* **2005**, *102*, 640.
[9] S. Hornemann, R. Glockshuber, *Proc. Natl. Acad. Sci. USA* **1998**, *95*, 6010.
[10] S. B. Prusiner, *Science* **1991**, *252*, 1515.
[11] I. V. Baskakov, G. Legname, M. A. Baldwin, S. B. Prusiner, F. E. Cohen, *J. Biol. Chem.* **2002**, *277*, 21140.
[12] D. S. Wishart, C. G. Bigam, A. Holm, R. S. Hodges, B. D. Sykes, *J. Biomol. NMR* **1995**, *5*, 67.
[13] S. Schwarzinger, G. J. A. Kroon, T. R. Foss, J. Chung, P. E. Wright, H. J. Dyson, *J. Am. Chem. Soc.* **2001**, *123*, 2970.
[14] J. A. Marsh, V. K. Singh, Z. Jia, J. D. Forman-Kay, *Protein Sci.* **2006**, *15*, 2795.
[15] J. Klein-Seetharaman, M. Oikawa, S. B. Grimshaw, J. Wirmer, E. Duchardt, T. Ueda, T. Imoto, L. J. Smith, C. M. Dobson, H. Schwalbe, *Science* **2002**, *295*, 1719.
[16] E. S. Collins, J. Wirmer, K. Hirai, H. Tachibana, S. Segawa, C. M. Dobson, H. Schwalbe, *ChemBioChem* **2005**, *6*, 1619.
[17] G. D. Rose, A. R. Geselowitz, G. J. Lesser, R. H. Lee, M. H. Zehfus, *Science* **1985**, *229*, 834.
[18] P. Hortschansky, V. Schroeckh, T. Christopeit, G. Zandomeneghi, M. Fändrich, *Protein Sci.* **2005**, *14*, 1753.
[19] R. Gerber, A. Tahiri-Alaoui, P. J. Hore, W. James, *Protein Sci.* **2008**, *17*, 537.
[20] Y. Ohhashi, Y. Hagihara, G. Kozhukh, M. Hoshino, K. Hasegawa, I. Yamaguchi, H. Naiki, Y. Goto, *J. Biochem.* **2002**, *131*, 45.
[21] L. M. Herrmann, B. Caughey, *NeuroReport* **1998**, *9*, 2457.
[22] A. K. Das, M. G. B. Drew, D. Haldar, A. Banerjee, *Org. Biomol. Chem.* **2005**, *3*, 3502.
[23] N. J. Cobb, F. D. Sönnichsen, H. Mchaourab, W. K. Surewicz, *Proc. Natl. Acad. Sci. USA* **2007**, *104*, 18946.
[24] N. J. Cobb, A. C. Apetri, W. K. Surewicz, *J. Biol. Chem.* **2008**, *283*, 34704.
[25] J. Ziegler, C. Viehrig, S. Geimer, P. Rösch, S. Schwarzinger, *FEBS Lett.* **2006**, *580*, 2033.
[26] M. L. DeMarco, V. Daggett, *Proc. Natl. Acad. Sci. USA* **2004**, *101*, 2293.
[27] T. Hart, L. L. P. Hosszu, C. R. Trevitt, G. S. Jackson, J. P. Waltho, J. Collinge, A. R. Clarke, *Proc. Natl. Acad. Sci. USA* **2009**, *106*, 5651.
[28] J. Collinge, *Annu. Rev. Neurosci.* **2001**, *24*, 519.
[29] S. Liemann, R. Glockshuber, *Biochemistry* **1999**, *38*, 3258.

